Tampering Dynamics

Nicholas C. GEORGANTZAS
Director, System Dynamics Consultancy
Fordham University Business Schools
113 West 60th Street, Suite 617-D
New York, NY 10023-7484, USA
Tel.: (212) 636-6216, Fax: (212) 765-5573
E-mail: georgantzas@fordham.edu

Joyce N. ORSINI
Director, Deming Scholars MBA
Fordham University Business Schools
33 West 60th Street, Suite 417
New York, NY 10023-7471, USA
Tel.: (212) 636-6219, Fax: (212) 636-7303
E-mail: orsini@fordham.edu

Abstract—Tampering can cause many of the tragedies that people and organizations increasingly face. To show pervasive forms of tampering, Deming used a funnel experiment, which quality researchers and practitioners now use to show the dysfunctional effects of not using statistical process control (SPC) charts. Interspersed with real-world tampering examples, this paper presents a system dynamics model of the funnel experiment, useful for reproducing Sparks & Field's (2000) SPC charts and statistical tests. The results also show multi-dimensional vistas of location probability and Theil's (1966) inequality statistics, plus an entropy-based view of tampering. System dynamics allows looking at the experiment causally, as opposed to merely looking at coincidental, due to randomness, SPC charts and entropy (uncertainty) measures. Looking under the hood, so to speak, one can see how the circular, feedback-loop relations among variables in the funnel experiment system produce assumption-violating dynamics as multiple feedback loops determine system behavior. Enhancing SPC with system dynamics can help detect, explain and prevent tampering with the very processes that managers must manage.

Keywords: assumptions, Deming, entropy, feedback, funnel experiment, Shewhart charts, simulation, statistical process control (SPC), system dynamics, tampering, uncertainty

Remember the *Tylenol Scare*? That tampering nightmare (Beck et al. 1982) was just one of the tragedies that made Mitroff & Kilmann (1984) look at the threats governmental, industrial, educational and health-care organizations face today. Only to see that psychopathology, sabotage and terrorism have become commonplace. Despite federal anti-tampering laws, terrorists, saboteurs and psychopaths continue committing such crimes, medical researchers fiddle with genes (August et al. 2002) and malicious troublemakers adjust, negate and remove pollution control equipment from factories and motor vehicles. To build wealth fast, managers too engage secretly or improperly in shady transactions and often meddle, mix up, rig and tinker with the very processes they are supposed to manage (Deming 2000a&b).

Look at *Enron*, for example. After a one-year old investigation, not one *Enron* manager has gone to jail (Dobbs 2002). Governments always tamper with the economy to talk up markets, but investors do not come back until they see real reforms, accountability and earnings. While ours, according to Dobbs (2002), "fails to assure them that is serious about choking off corporate fraud," the *PricewaterhouseCoopers* data show that, from 2000 to 2001, annual securities-tampering litigation in USA increased by 240.3 percent (O'Connor 2002).

According to *Merriam-Webster's Collegiate Dictionary* (2001), 'tampering' entails carrying on underhand or improper negotiations (as by bribery) and interfering so as to weaken, to make something worse. In management, *tampering* entails reacting to common-cause variation or randomness in a process as if it were special-cause variation. Every time a manager mistakes randomness for special-cause variation, tampering makes processes, i.e., *Merriam-Webster's* 'something', worse too. Managers who understand that tampering with a process is harmful will

let the process run and study it (Latzko & Saunders 1995). But the profound knowledge required to stop tampering (a) has no substitute and (b) is not automatic (Deming 2000a&b). It takes wisdom to manage the uncertainty that leads to tampering with a process. And managing uncertainty must be learnt; must be led (Georgantzas & Acar 1995).

According to Deming (2000a&b), managers tamper with processes because they are trained to do so. They react to each rise in performance as if things were improving and react to each dip in performance as if things were beginning to fall apart. Typically, nothing has changed at all. What managers react to is common randomness, which pervades all business systems and processes as "a measure of our ignorance" (Sterman 2000, p. 127).

It was Walter A. Shewhart of the *Bell Telephone Laboratories* who first used statistics for quality control. Shewhart's 16 May 1924 memorandum featured the very first sketch of a modern control chart (*cf.* Schultz 1994, p. 5). Shewhart worked on and improved his approach until his 1931 book (Shewhart 1980) set the tone for statistical process control (SPC). To tell between chance and assignable causes or variation, he created a method to distinguish one type of variation from the other. Following Shewhart, Deming (2000a&b) refers to 'common' and 'special' causes of variation. *Common* causes are inherent in a process. *Special* causes are rare events that require immediate action. When a machine starts producing defects consistently, for example, it must be taken off line for repair. But eighty to ninety percent of product and service variation is due to common causes, endemic to a process. The only way to reduce common variation is to redesign the process itself.

To show subtle but pervasive forms of tampering with stable processes, Deming (2000a&b) used a funnel experiment for which he credits Dr. Lloyd S. Nelson, Director of Statistical Methods, *Nashua Corporation* (Deming 2000a, p. 20). Its well-established four rules determine the funnel and marble *dynamics*, i.e., behavior through time. MacGregor (1990) used the funnel experiment to show the value of control versus no control for a drifting process mean, Gunter (1993) for experimental design and Sparks & Field (2000) to check their SPC chart assumptions.

Sparks & Field see in the funnel experiment a useful tool for quality trainers to show practitioners how to use SPC charts correctly. Inappropriate charts lead to excessive, unnecessary adjustment of a process, time lost in looking for nonexistent special causes, or to a belief that the process is out of control because of the false signaling of special causes. Well aware that decisions based on 'black-box' SPC charts can be incorrect (Field & Sparks 1995), Sparks & Field (2000) present a unidimensional analysis of the funnel experiment as a means of training workers to become discerning SPC users. Sparks & Field also address practitioner concerns about the behavior that the funnel experiment SPC charts produce.

Interspersed with real-world tampering examples, the funnel experiment overview below reiterates the practitioner concerns that Sparks & Field (2000) address because of their educational value. The model description section then presents a two-sector system dynamics (Forrester 1958 & 1961) model of the funnel experiment. The results show the model's usefulness as it helps replicate Sparks & Field's (2000) SPC charts and statistical tests. Next, however, the paper goes beyond the unidimensional analysis of SPC charts. It adds three-dimensional graphs of location probability and Theil's (1966) inequality statistics (TIS). Also, it measures location uncertainty using Shannon's information entropy (Shannon & Weaver 1949) and thereby shows an entropy (uncertainty) based view of the funnel experiment.

The 3D graphs, TIS and the discerning entropy-based view of the funnel experiment are some of the benefits from extending "the necessary mathematical framework" of Sparks & Field (2000, p. 292) with a system dynamics model. System dynamics, the study of cause and effect

through time, allows looking at Deming's experiment causally, as opposed to merely looking at coincidental, due to randomness, SPC charts and entropy measures. Looking under the hood, so to speak, the paper shows how the circular, feedback-loop relations among variables in the funnel experiment system produce assumption-violating dynamics as multiple feedback loops determine system behavior. Enhancing SPC with system dynamics can help detect, explain and prevent tampering with the very processes that managers must manage.

Deming's funnel experiment and quality practitioner concerns

An apparatus that demonstrates Deming's funnel experiment includes a mobile stand that holds a funnel at a fixed height above a gridded paper pad (Fig. 1). The point (0, 0) on the gridded pad designates the target. Imagine dropping the marble down the funnel. The marble rolls down inside and out the funnel in a random fashion. *Friction*, *gravity* and *harmonics* are some of the natural forces acting on the marble to produce common-cause, i.e., random, variation (Latzko & Saunders 1995, p. 151).

Figure 1 An apparatus for the Deming- Nelson funnel experiment

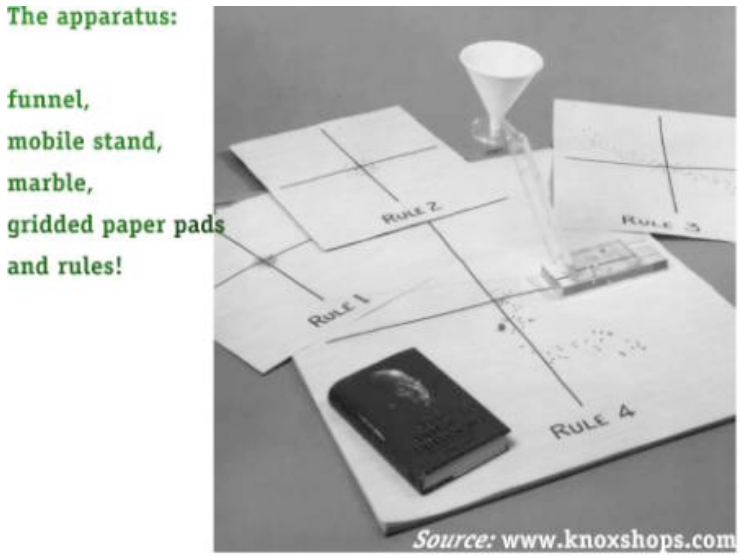

With the funnel clamped to its steady stand, the marble drops on the gridded pad and rolls until it stops somewhere near the target. A pen easily marks the spot where the marble comes to a rest. When repeatedly dropped through the funnel, the marble does not always land nor does it come to a rest on the same spot. Natural forces make it drop and stop randomly around the target. Performing the funnel experiment requires dropping the marble through the funnel multiple times, while one of the four rules on Table 1a determines the funnel's aiming point (Deming 2000a&b, Latzko & Saunders 1995, Sparks & Field 2000).

Rule 1 means no tampering (Table 1a). The funnel remains aimed at the target. Its position is the same for each drop, "producing a stable distribution of points and a minimum variance on any diameter drawn through the target" (Deming 2000a, p. 329).

Rule 2 implies reacting to an individual data point by correcting in an equal and opposite direction. Adjusting the position of a gun after firing one shot at a target is one example of this form of tampering. Another example is the tampering that takes place with the thermostat in a conference room. Someone feels hot when coming into the room from the hallway and, on the basis of this one data point, how the room feels upon entering it, adjusts the thermostat. That per-

son is changing the system based on that one point. Someone else comes in later, when the room is on the cool side of its cycle, and tampers the system up to a higher temperature. Over the course of the day these tampering adjustments increase the variation of the temperature in the room. Back to the funnel experiment, Rule 2 produces stable results, but the variance of the distribution of points along any diameter drawn through the target will, under Rule 2, be double the expected variance under Rule 1 (Deming 2000a, Sparks & Field 2000).

Table 1 The Deming-Nelson funnel experiment (a) rules and (b) practitioner questions

(a)	*Rule*	*Simplified rule description* adapted from Deming (2000a, p. 328)*
	1	Keep funnel aimed at the target (**no tampering**)
	2	Move funnel from **its last position** to compensate for last error
	3	Move funnel from **the target** to compensate for last error
	4	Move funnel right over the previous drop location
(b)	*Question*	*Quality practitioner questions* adapted from Sparks & Field (2000, p. 292)
	1	Under Rule 2, why does the $\bar{x}$ chart hug the centerline?
	2	Why does the Rule 3 $\bar{x}$ chart hug the centerline even more?
	3	Why does the Rule 3 $\bar{x}$ chart develop a strong alternating behavior for odd sample sizes?
	4	Why do later vales on the Rule 3 $\bar{x}$ chart with odd sample sizes deviate more from the centerline than do earlier values? Why is this behavior not apparent for even sample sizes?
	5	Why does the Rule 4 $\bar{x}$ chart behave as if very out of control?
	6	Given the processes under the four different rules, what are the appropriate charts?

* In addition to crediting Dr. Lloyd S. Nelson for the funnel experiment idea, Deming attributes experimental results to Lord Rayleigh's work on *vibrations* and *theory of sound*, and to Dr. Frank S. Grubbs (Grubbs 1983) for *optimum convergence to the target* (Deming 2000a, p. 329).

Although Sparks & Field (2000) do a remarkable job in answering quality practitioner questions from a statistical viewpoint, the simple system dynamics model of the funnel experiment presented here can still offer insight in answering Questions 1, 2 and 5.

Rule 3 makes one forget about the target and react only to the last event that happens. The system explodes as the marble rest points eventually move away farther and farther in opposite direction from the target, in a symmetrical bow-tie pattern; an accelerating swing from one direction to another. Escalating warfare is an example of Rule 3 tampering. One side increases its nuclear arms. The other sides increase theirs. The first side then reacts by increasing its arms, and so on. Zero-based budgeting, price wars between stores, promotional competition, shouting matches, one-upmanship and the wildcard interest rates of the late 1970s are good examples too. Usually, escalation persists until the system explodes or outside intervention occurs or one side quits, surrenders or goes out of business. In the case of wildcard interest rates, outside intervention by a regulatory agency can bring an end to irrationally escalating rates.

Rule 4 abandons all hope of hitting the target and tries instead to be consistent with the last outcome. The marble eventually moves farther and farther from the target as if executing a random walk under Brownian motion. The 'telephone game' that children play is a good example of this tampering rule. One person whispers a story to another, who in turn whispers it to another, who again whispers it to another, and so on, until the last person says out loud what s/he heard. When the first person announces what was whispered initially, then everyone laughs at how the

story has completely changed in the game's quiet retelling. Each person whispers the story based on the soft whisper by the person before, thereby creating a clear instance of tampering under Rule 4 (Table 1a). The corporate version entails rumors that spread throughout a company. With each repetition, the story changes somewhat, often wandering off farther from the truth with each retelling. Another example is on-the-job training by employees, with each new employee training the next. A training center avoids this type of tampering. Similarly, in real estate, a construction firm draws blueprints before constructing a building. When it makes an addition to the building two years later, its engineers redraw the blueprints to include the new addition. A year later, when four offices are combined to create a new conference room, new blueprints are made from the last set. Through time, small mistakes accumulate. Based on the last set created, new blueprints begin to differ substantially from the actual building and new mistakes get added with new iterations.

Under Rule 1 (no tampering), each marble drop is independent of any other drop. So, the autocorrelation, covariance and the process mean for Rule 1 are all zero (Sparks & Field 2000). Under Rules 2 through 4, however, the aim for each drop depends on where the marble came to a rest at the previous drop. Under Rules 2 and 3, the process mean remains zero, but it does change under Rule 4, signaling a location change. Sparks & Field (2000) show exact autocorrelation and variance results for Rules 2 through 4 and how these three rules violate their assumptions about normality. Subsequently, they address the questions of Table 1b by comparing SPC chart limits.

Shewhart (1980) does not require that distribution characteristics be plotted on SPC charts and shows that normality is not essential. If normality were essential, then SPC charts would not work as well as they do. Supporting Shewhart's experimental results with the *Triangular* and the *Uniform* distributions, Wheeler's (2000) data from 1,143 *heap*-, *J*- and *U*-shaped probability distributions confirm that deviations from normality have little effect on SPC chart parameters. Bolstered by the *Central Limit Theorem*, however, some statisticians deem normality desirable, if not outright required, as Sparks & Field (2000) argue.

To answer the practitioner questions of Table 1b, Sparks & Field show a unidimensional version of Deming's funnel experiment. They mathematically model each of its four rules (Table 1a), which they use to generate experimental data using a computer. From their simulation data, Sparks & Field (2000) then plot R and $\bar{x}$ charts, linking the behavior of their charts to the practitioner questions of Table 1b.

The two-sector system dynamics model below also generates experimental data using a computer. Based on the simulation data, the results section first replicates Sparks & Field's (2000) unidimensional analysis and then checks their statistical assumptions. It adds three-dimensional views of the marble's location probability for Rules 1 through 4 and Theil's (1966) inequality statistics (TIS) for Rules 2 through 4 compared to Rule 1. Also, it measures entropy (uncertainty) about the marble's location for Rules 1 through 4 using Shannon's information entropy formula, thereby showing an entropy-based view of the Deming-Nelson funnel experiment. After Boltzmann's and von Neumann's work on statistical mechanics, Shannon defined information entropy as:

$$U = -k\sum_{i=1}^{n} p_i \log p_i, \qquad (1)$$

where i runs over all possible outcomes n, p_i is the probability of finding the marble in state i, and k is a positive constant (Shannon & Weaver 1949).

Model description

Extending Sparks & Field's (2000) work on the funnel experiment with system dynamics hinges on two bases. *First*, Deming's (2000b) *System of Profound Knowledge*, which integrates systems, statistics, knowledge theory and psychology, begins with building appreciation for a system. *Second*, Deming said: "Until you draw a flow diagram, you do not understand you business" (*cf.* Schultz 1994, p. 21). System dynamics does use stock and flow diagrams to depict relations among variables in a system. A fundamental tenet of system dynamics is that the structure of relations among variables in a system gives rise to its behavior (Sterman 2001, p. 16). Figure 2 shows the stock and flow diagram of the funnel (Xf, Yf) and marble (Xm, Ym) location sector, reproduced from the simulation model built with *iThink*® *Analyst* 7 (Richmond et al. 2001).

There is a one-to-one association between the model diagram of Fig. 2 and its equations (Table 2). Like the diagram of Fig. 2, the equations are also the actual output from *iThink*®. Building the model entailed first diagramming the experiment's structure on the glass of a computer screen and then specifying simple algebraic equations and parameter values. The software enforces consistency between the diagram and the equations, while its built-in functions help quantify parameters and variables pertinent to the funnel experiment rules, instigated with two switches (Fig. 2, and Eqs 2.15 and 2.16, Table 2).

In system dynamics, rectangles represent stocks or level variables that can accumulate, such as the funnel Xf and Yf coordinates on Fig. 2. Emanating from cloud-like sources and ebbing into cloud-like sinks, the double-line, pipe-and-valve-like icons that fill and drain the stocks represent flows or rate variables that cause the stocks to change. The pulse Xm outflow (right of Fig. 2), for example, bleeds dry the marble Xm stock after a pen marks the spot where the marble comes to a rest. Single-line arrows represent information connectors, while circular icons depict auxiliary converters where constants, behavioral relations or decision points convert information into decisions. Under Rule 2, for example, the change Ym flow depends on the funnel Yf coordinate stock, adjusted by the marble's random angle and random distance as it randomly rolls down inside and out the funnel.

Rule 1 requires that both switches equal zero to keep the funnel's position the same for each marble drop. Without tampering, the funnel stays aimed at the fixed (0, 0) target. As long as Rule 1 plays, the funnel's Xf and Yf coordinates (Eqs 2.1 and 2.2) retain their initial (INIT) zero value (Eqs 2.1.1 and 2.2.1). Only the Xm and Ym stocks (Eqs 2.3 and 2.4) and their associated flows and converters on Fig. 2 are active under Rule 1. Each marble drop entails generating a random angle between zero and 2π radians (Eq. 2.13) and a random distance between zero and one inch (Eq. 2.14). Together, the product of the random angle *cosine* (COS) and random distance then determines the change Xm inflow (Eq. 2.9), which feeds the marble Xm coordinate (Eq. 2.3). Similarly, the product of the random angle *sine* (SIN) and random distance determines the change Ym inflow (Eq. 2.11), which feeds the marble Ym coordinate (Eq. 2.4). "No tampering" (Deming 2000a, p. 328) means, however, independent marble drops (Sparks & Field 2000, p. 293). That is why the pulse Xm and pulse Ym outflows (Eqs. 2.10 and 2.12) are quick to completely drain the marble Xm and Ym stocks (Eqs 2.3 and 2.4), respectively, after a pen marks the spot where the marble comes to a rest.

Rule 2 calls for setting switch 1 = –1 to enable the funnel to move, erroneously correcting in an equal but opposite (–) direction in response to an individual (Xm, Ym) data point. But switch 2 again equals zero (Eq. 2.16) to let the funnel Xf and Yf coordinate stocks (Eqs 2.1 and 2.2) accumulate. Deming calls the accumulation of the funnel Xf and Yf coordinate stocks

"Memory 1" in his description of Rule 2 (Deming 2000a, p. 328). With the aim for each drop now dependent on where the marble came to a rest at the previous drop, the cumulative Xf and Yf coordinates affect the change Xm and change Ym inflows (Eqs 2.9 and 2.11). Feeding these flows with the previous drop location's cumulative data means adding to and actually doubling the variance of the marble's Xm and Ym coordinates (Sparks & Field 2000, p. 293).

Figure 2 The funnel (Xf, Yf) and marble (Xm, Ym) location sector

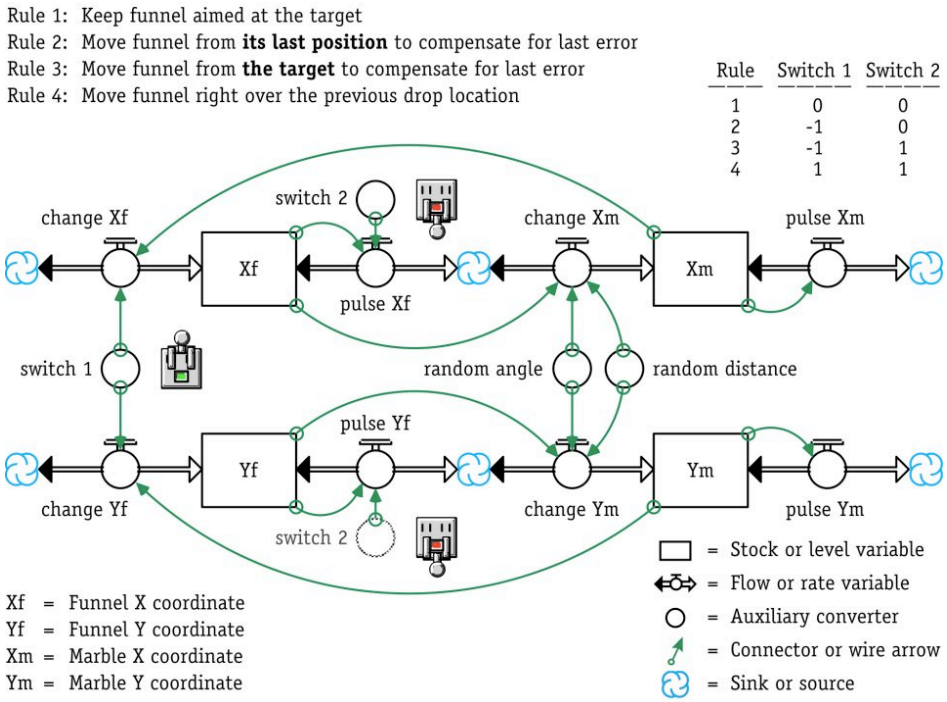

Table 2 The funnel (Xf, Yf) and marble (Xm, Ym) location sector equations

Stocks: level or state variables	*Eq. #*
Xf(t) = Xf(t – dt) + (change Xf – pulse Xf) * dt	(2.1)
INIT Xf = 0 {funnel X coordinate; unit = inch}	(2.1.1)
Yf(t) = Yf(t – dt) + (change Yf – pulse Yf) * dt	(2.2)
INIT Yf = 0 {funnel Y coordinate; unit = inch}	(2.2.1)
Xm(t) = Xm(t – dt) + (change Xm – pulse Xm) * dt	(2.3)
INIT Xm = 0 {marble X coordinate; unit = inch}	(2.3.1)
Ym(t) = Ym(t – dt) + (change Ym – pulse Ym) * dt	(2.4)
INIT Ym = 0 { marble X coordinate; unit = inch}	(2.4.1)
Flows: rate variables	
change Xf = switch 1 * Xm {unit = inch / drop; t = TIME = 200 drops or trials}	(2.5)
pulse Xf = PULSE(switch 2 * Xf, 1, 1) {unit = inch / drop}	(2.6)
change Yf = switch 1 * Ym {unit = inch / drop}	(2.7)
pulse Yf = PULSE(switch 2 * Yf, 1, 1) {unit = inch / drop}	(2.8)
change Xm = Xf + COS(random angle) * random distance {unit = inch / drop}	(2.9)
pulse Xm = PULSE(Xm, 1, 1) {unit = inch / drop}	(2.10)
change Ym = Yf + SIN(random angle) * random distance {unit = inch / drop}	(2.11)
pulse Ym = PULSE(Ym, 1, 1) {unit = inch / drop}	(2.12)
Converters: auxiliary variables and constants	
random angle = RANDOM(0, 2 * PI) {unit = radian / drop}	(2.13)
random distance = RANDOM(0, 1) {unit = inch / drop}	(2.14)
switch 1 = 0 {unit = dimensionless}	(2.15)
switch 2 = 0 {unit = dimensionless}	(2.16)

Rule 3 again makes the aim for each drop depend on where the marble came to a rest at the previous drop. But there is no funnel stock accumulation now; "No memory" (Deming 2000a, p. 328). Setting switch 2 = 1 activates the pulse Xf and pulse Yf outflows (Eqs 2.6 and 2.8) and thereby eliminates the funnel Xf and Yf coordinate accumulation. Once activated, the pulse Xf and pulse Yf outflows render the funnel Xf and Yf coordinates memoryless. The lack of memory makes one forget about the (0, 0) target and react only to the last event. Like an escalating warfare, the marble consecutive rest points eventually move away farther and farther in opposite direction from the target, in an accelerating swing from one direction to another. The marble Xm and Ym coordinate variance rises with each marble drop (Sparks & Field 2000, p. 293).

Rule 4 not only wants the funnel Xf and Yf coordinates memoryless too, but completely abandons all hope of hitting the target and tries instead to be consistent with the last outcome. Like the *muddling through* of the telephone game and the *logical incrementalism* some strategy theorists prescribe (e.g., Mintzberg 1994 and Quinn 1980), the marble eventually moves farther and farther from the target as if executing a random walk. Its Xm and Ym coordinate variance rises proportionally with each marble drop as the aim for each drop again depends on where the marble came to a rest at the prior drop (Sparks & Field 2000, p. 293).

Marble location probability (Pml) and entropy/uncertainty (Uml) sector

Computing the entropy (uncertainty) about the marble location with Eq. 1 is equivalent to assessing its state after each drop. To make it so requires gridding or tiling a paper pad (Fig. 1) and then computing location probabilities by counting how frequently the marble *hits* each tile, i.e., comes to a rest there. The marble location probability (Pml) and uncertainty (Uml) sector computes the uncertainty about marble location after each drop (Fig. 3 and Table 3).

One can choose a tiling scheme empirically after observing running simulations. A 15×15 tiling would, for example, require a total of 225 array elements, but Table 3 gets away with only 49, thanks to its 7×7 tiling scheme. Extreme cases, i.e., a 1×1 grid, notwithstanding, grid resolution has no effect on the shape of the entropy/uncertainty increase, but simply reduces time to saturation, i.e., Uml reaching its upper bound of one (Georgantzas 2002). It is possible to compute location probabilities by averaging over multiple simulation runs, but the model sector of Fig. 3 computes marble location probabilities and uncertainty (entropy) dynamically.

Initialized at zero (Eq. 3.1.1), the one-dimensional arrayed Marble Drops[·] stock (Eq. 3.1) counts how many times the marble hits each tile of the superimposed 7×7 tiling scheme. Each time the marble hits the *first* tile, for example, the change Marble Drops[1] inflow array (3.3) adds a hit to the Marble Drops[1] array (3.1). Subsequently, the Pml[1] converter array (3.102) computes the probability of the marble coming to a rest on the *first* tile as the dimensionless ratio of the Marble Drops[1] stock array value over the total drops array sum (3.151). Adding a one to this array sum converter prevents its dividing by zero because of empty tiles.

While the arrayed Pml[·] converters (Eqs 3.102 through 3.150) compute marble location probabilities, the log Pml[·] converters (Eqs 3.53-3.101) calculate their respective logarithms. Together, the probabilities, their logarithms and the total marble location probability (total Pml) array sum (3.152) determine the change Uml (3.52) inflow, which feeds the marble location entropy/uncertainty Uml stock (3.2), using Shannon's entropy formula (Eq. 1). Shannon's positive constant k gets smaller as Uml increases and its difference from the total Pml auxiliary converter (3.152) decreases. Dividing the reported marble location uncertainty by $\log_{10}(10)$ in the change Uml flow makes the logarithm base irrelevant (Eq. 3.52).

Figure 3 The marble location probability (Pml) and entropy/uncertainty (Uml) sector

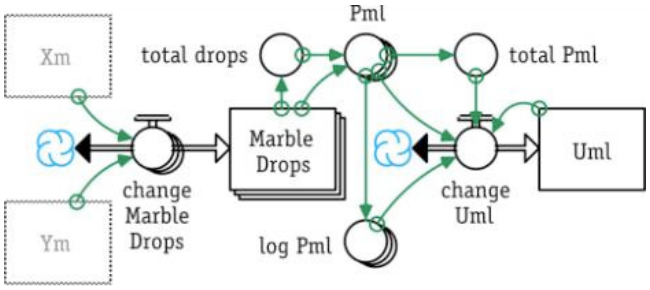

Table 3 The marble location probability (Pml) and uncertainty (Uml) sector equations

Stocks: level or state variables	*Eq. #*
Marble Drops[·](t) = Marble Drops[·](t – dt) + (change Marble Drops[·]) * dt	(3.1)
INIT Marble Drops[·] = 0 {unit = hit}	(3.1.1)
Uml(t) = Uml(t – dt) + (change Uml) * dt	(3.2)
INIT Uml = 0 {unit = dimensionless}	(3.2.1)
Flows: rate variables	
change Marble Drops[1] = IF (–7 <= Xm AND (Xm < –5) AND (–7 <= Ym) AND (Ym < –5)) THEN (1) Else (0) {unit = hit / drop}	(3.3)
change Marble Drops[2] = IF (–5 <= Xm AND (Xm < –3) AND (–7 <= Ym) AND (Ym < –5)) THEN (1) Else (0) {unit = hit / drop}	(3.4)
⋮	⋮
change Marble Drops[49] = IF (5 <= Xm AND (Xm < 7) AND (5 <= Ym) AND (Ym < 7)) THEN (1) Else (0) {unit = hit / drop}	(3.51)
change Uml = (total Pml – Uml) * (– ((Pml[1] * log Pml[1] + Pml[2] * log Pml[2] + . . . + Pml[49] * log Pml[49]) / LOG10(10))) {unit = dimensionless / drop}	(3.52)
Converters: auxiliary variables and constants	
log Pml[1] = IF (Pml[1] = 0) THEN (0) ELSE (LOG10(Pml[1])) {unit = dimensionless}	(3.53)
log Pml[2] = IF (Pml[2] = 0) THEN (0) ELSE (LOG10(Pml[2])) {unit = dimensionless}	(3.54)
⋮	⋮
log Pml[49] = IF (Pml[49] = 0) THEN (0) ELSE (LOG10(Pml[49])) {unit = dimensionless}	(3.101)
Pml[1] = Marble Drops[1] / total drops {unit = dimensionless}	(3.102)
Pml[2] = Marble Drops[2] / total drops {unit = dimensionless}	(3.103)
⋮	⋮
Pml[49] = Marble Drops[49] / total drops {unit = dimensionless}	(3.150)
total drops = ARRAYSUM(Marble Drops[*]) + 1 {unit = hit}	(3.151)
total Pml = ARRAYSUM(Pml[*]) {unit = dimensionless}	(3.152)

Simulation results

The results here entail setting the *iThink*® run specs as follows: Euler's integration method with simulation length TIME ∈ [1, 200] (drops) and computation interval $dt = 1$. These settings match Sparks & Field's (2000) specifications. The phase plots of Fig. 4 show how marble (Xm, Ym) location patterns form under Rules 1 through 4. Although Sparks & Field do not show any phase plots, the ones on Fig. 4 are similar to those of Deming (2000a, p. 328) and Latzko & Saunders (1995, pp. 151-154).

Rule 1 (no tampering) keeps the funnel stationary, aimed at the (0, 0) target, as the marble drops. The marble then rolls until it stops somewhere near the target. As the marble comes to a rest near the target for 200 successive drops, its marked rest points form a circular gradient pattern (top left, Fig. 4). This circular pattern is the result of a process in control with common-cause or random variation.

Figure 4 Marble location (Xm, Ym) phase plots for Rules 1 through 4 (200 drops per rule)

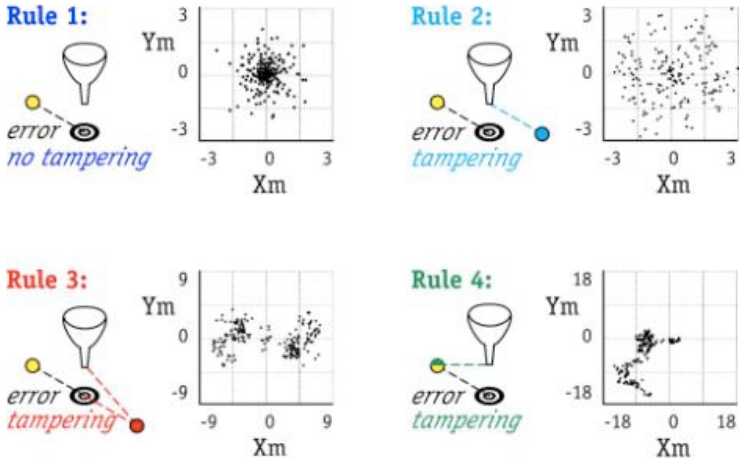

Rule 2 erroneously compensates for the last error in an equal but opposite (–) direction in response to the marble (Xm, Ym) location data. The switch 1 = –1 value enables the funnel to move now, but switch 2 still equals zero, letting the funnel Xf and Yf stocks accumulate. The top right of Fig. 4 shows that Rule 2 produces stable results, but the variance of the distribution of points along any diameter drawn through the target is double the expected variance under Rule 1 (Deming 2000a and Sparks & Field 2000).

Rule 3 makes the aim for each drop depend on where the marble came to a rest at the previous drop, but without any stock accumulation; no memory now. The lack of memory due to switch 2 = 1 causes the marble rest points to move away farther and farther in opposite direction from the target. Like those irrational, escalating price wars between stores, the funnel's and marble's accelerating swing from one direction to another form the symmetrical bowtie-like pattern on the lower left of Fig. 4.

Rule 4 causes the marble rest points to move farther and farther from the target as if executing a random walk under Brownian motion. The phase plot on the lower right of Fig. 4 shows a typical instance of tampering under Rule 4. Not only the funnel Xf and Yf coordinates are memoryless now but, much like muddling through and logical incrementalism proponents and managers, Rule 4 abandons all hope of hitting the target and tries instead to be consistent with the last outcome. The Xm and Ym coordinate variance rises proportionally with each marble drop as the aim for each drop again depends on where the marble came to a rest at the previous drop (Sparks & Field 2000, p. 293).

Statistical behavior and test reproduction

Sparks & Field's (2000) unidimensional results entail 200 simulated consecutive marble drops through the funnel under each rule. They then take 50 successive samples of size $n = 4$ from their 200 marble drops and plot R (range) and $\bar{x}$ (x-bar) charts. Applied to the data of Fig. 4, Sparks & Field's sampling procedure produces the R and $\bar{x}$ charts of Fig. 5, Fig. 6 and Fig. 7.

The normality assumptions Sparks & Field (2000, p. 295) choose to test for are:

R chart: sample values are *both* independent and approximately normally distributed with constant variance.

$\bar{x}$ chart: sample values are independent and their *means* are approximately normally distributed with constant variance.

Figure 5 R (range) charts for Rules 1 through 4 (sample size n = 4)

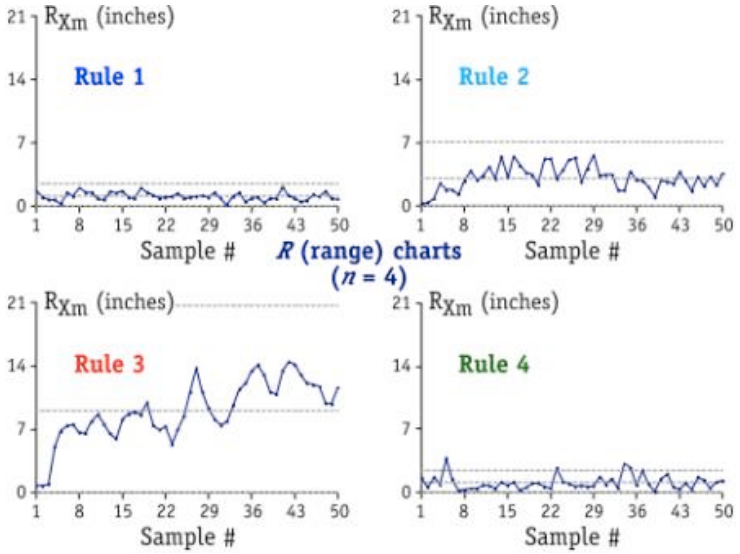

Figure 6 $\bar{x}$ (x-bar) charts for Rules 1 through 4 (sample size n = 4)

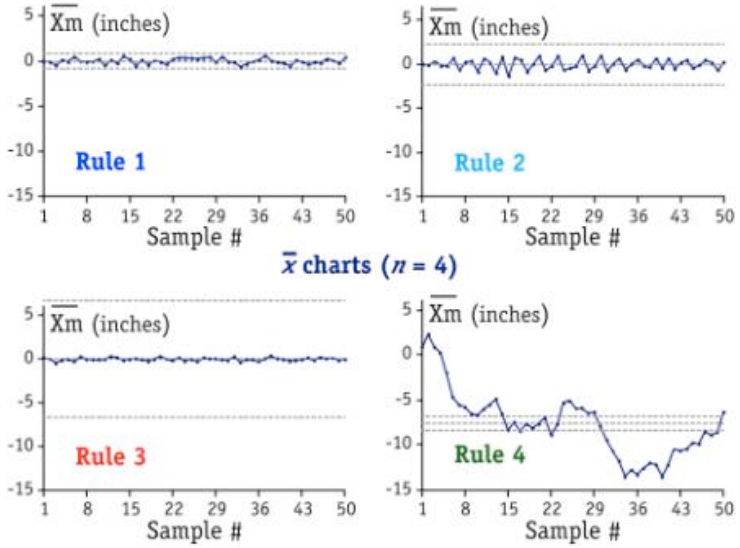

Figure 7 R (range) and $\bar{x}$ (x-bar) charts for Rule 3 (sample size n = 5)

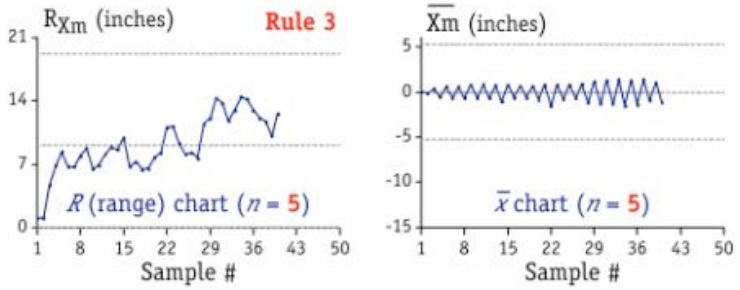

The between values *correlation coefficient* (r), which measures the degree to which data co-vary, gives the lag j sample *autocorrelation coefficient* (r_j) between lagged samples. A zero autocorrelation means uncorrelated values. If uncorrelated values are also normally distributed,

then they are independent. To check for autocorrelation and independence, Sparks & Field (2000, p. 296) compute the autocorrelations between lagged samples that the funnel experiment rules generate. Using this approach, Fig. 8 shows the Xm lag j autocorrelations r_j that Rules 1 through 4 generate (j = 0, 1, …, 9). After lag zero, all Rule 1 autocorrelations are nonsignificant (top left, Fig. 8). But the rest of Fig. 8 shows significant Xm autocorrelations after lag zero for Rules 2, 3 and 4, indicating that the adjacent Xm values these rules generate are dependent.

Figure 8 The lag j autocorrelations r_j for Xm, Rules 1 through 4 (j = 0, 1, …, 9)

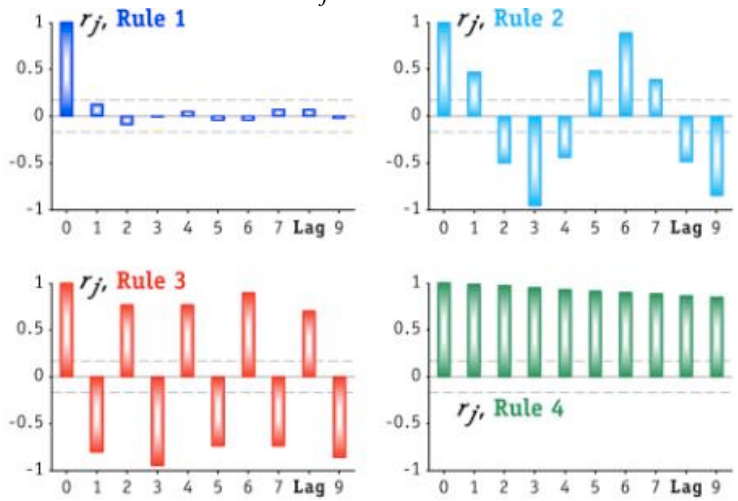

The way Sparks & Field (2000, p. 296) check for the constant variance assumption in individual sample values entails comparing parallel boxplots for the first half of the data in a sample with the other half. Using their approach, Fig. 9 shows the parallel boxplots of the marble Xm coordinate data for Rules 1 through 4. It is worth noting that while Rules 3 and 4 both show increasing variance (lower panel, Fig. 9), Rules 1 and 2 do not (top panel, Fig. 9). The results of Fig. 9 confirm those of Sparks & Field. While Rules 1 and 2 produce data with homogeneous variance, the Rule 3 and 4 data are likely to show variance heterogeneity.

Figure 9 Parallel boxplots of Xm for Rules 1 through 4 (200 drops per rule)

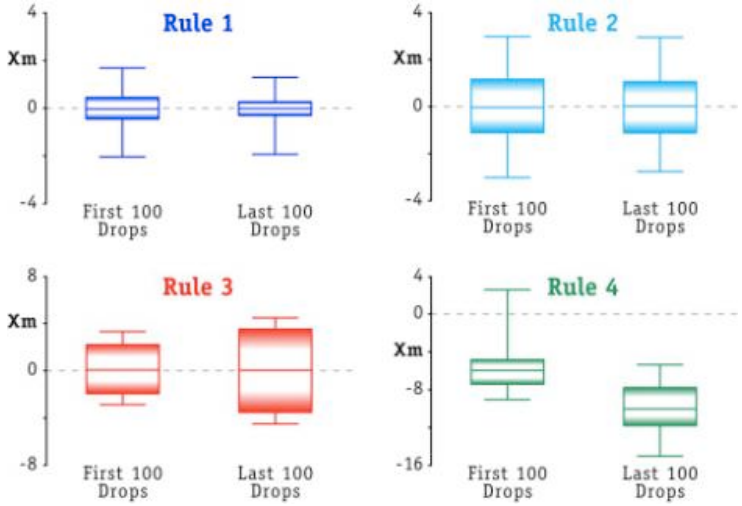

To test for the variance homogeneity and normality assumptions, Sparks & Field use Wilk & Gnanadesikan's (1968) Q-Q plot, which computes the ith quintile from standard normal tables.

When both the variance homogeneity and the normality assumptions hold, then the Q-Q plot is linear. Deviations from linearity mean outlying data, variance heterogeneity or non-normality. Figure 10 shows the Q-Q plots for the individual sample data of the marble Xm coordinate under Rules 1 through 4. The Q-Q plots for Rules 1 and 2 (top panel, Fig. 10) show normally distributed data with homogeneous variances. But the Rule 3 and Rule 4 Q-Q plots (lower panel, Fig. 10) show sample data either not normally distributed or with heterogeneous variance.

Figure 10 Q-Q plots of marble X coordinate (Xm) for Rules 1 through 4 (200 drops per rule)

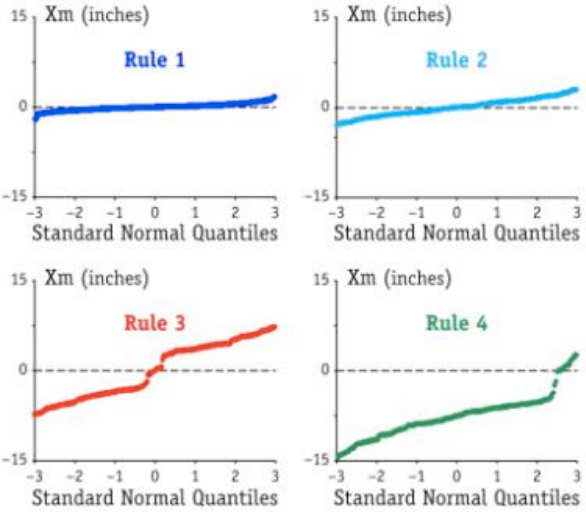

Answers to quality practitioner questions with statistics

Statistical process control charts like the ones Fig. 5, Fig. 6 and Fig. 7 show make quality practitioners ask the questions of Table 1b. To answer **Question 1**: «Under Rule 2, why does the $\bar{x}$ chart hug the centerline?» Sparks & Field explain that the large variance of tampering Rule 2 inflates the control limits of both the *R* (top right, Fig. 5) and the $\bar{x}$ (top right, Fig. 6) charts. But what causes the large variance under Rule 2? How does the structure of relations among variables in the funnel experiment system gives rise to dynamics that violates Sparks & Field's assumptions of independence and homogeneous variance?

In response to **Question 2**: «Why does the Rule 3 $\bar{x}$ chart hug the centerline even more?» Sparks & Field explain that the large variance of tampering Rule 3 inflates the control limits of both the *R* (lower left, Fig. 5) and $\bar{x}$ (lower left, Fig. 6) charts, causing them to hug the centerline. Again, why the large variance under tampering Rule 3? What causes it?

Sparks & Field (2000) answer all questions of Table 1b, at least from their perspective. The system dynamics model of the funnel experiment presented here can still offer insight in answering Questions 1, 2 and 5 (marked with the filled diamond symbol ' ' on Table 1b). In response to Question 3: «Why does the Rule 3 $\bar{x}$ chart develop a strong alternating behavior for odd sample sizes?» for example, there is little insight this simple model can add because, to keep it simple, SPC sampling and plotting procedures are external and posterior to the model.

To answer **Question 3** (Table 1b), Sparks & Field explain that because the sample means' autocorrelation is close to –1 for odd lags and +1 for even lags, the $\bar{x}$ values alternate above and below the centerline. Differences in the alternating behavior of the sample means are seen in comparing the sample size four ($n = 4$) $\bar{x}$ chart (lower left, Fig. 6) to its sample size five ($n = 5$) counterpart (right panel, Fig. 7). Their response to **Question 4** (Table 1b) is that, although *R* charts generally behave similarly for even and odd sample sizes (lower left of Fig. 5 and left

panel of Fig. 7), the sample size four ($n = 4$) means (lower left, Fig. 6) have a much smaller and constant variance than the variance of sample means with $n = 5$ (right panel of Fig. 7) for large i (number of marble drops) values (Sparks & Field 2000, p. 298).

In response to **Question 5**: «Why does the Rule 4 $\bar{x}$ chart behave as if very out of control?» Sparks & Field explain that the sample mean variance under Rule 4 increases with each marble drop. The larger the number of marble drops, the more the $\bar{x}$ chart centerline or process mean will differ from its zero target. The "increasing uncertainty" about $\bar{x}$ values as the marble drops increase, "together with the increased autocorrelation between these values explains why the [$\bar{x}$] values are likely to wander away from zero as i [the number of marble drops] increases" (Sparks & Field 2000, p. 298). But what causes the large variance of tampering Rule 4? How does the structure of relations among variables in the funnel experiment system give rise to dynamics that violates the "approach of using within-group variation to estimate the process variance [and] makes matters a great deal worse" (Sparks & Field 2000, p. 298)?

Sparks & Field conclude by answering **Question 6**. They recommend using "CUSUM charts of residuals for identifying special cause behavior particularly for processes that wander" (2000, p. 298).

Beyond unidimensional analysis: marble location probability (Pml)

The three-dimensional surface plots of the marble location probability (Pml) confirm the roughly normally distributed data with homogeneous variance under Rules 1 and 2 (top panel, Fig. 11). Naturally, since the marble Xm and Ym coordinates are two different variables, one must no longer talk of a normal distribution but, rather, of a bivariate normal distribution. And the tails of the bivariate normal distribution that Rule 2 produced (top right, Fig. 11) are fat. Indeed, they are much fatter than the tails of the bivariate normal distribution that Rule 1 produced (top left, Fig. 11). This corroborates Deming's (2000a) and Sparks & Field's (2000) argument that, under Rule 2, the variance of the distribution of points along any diameter drawn through the target is *double* the expected variance under Rule 1.

Figure 11 Marble location probability (Pml) for Rules 1 through 4 (2,000 drops per rule)

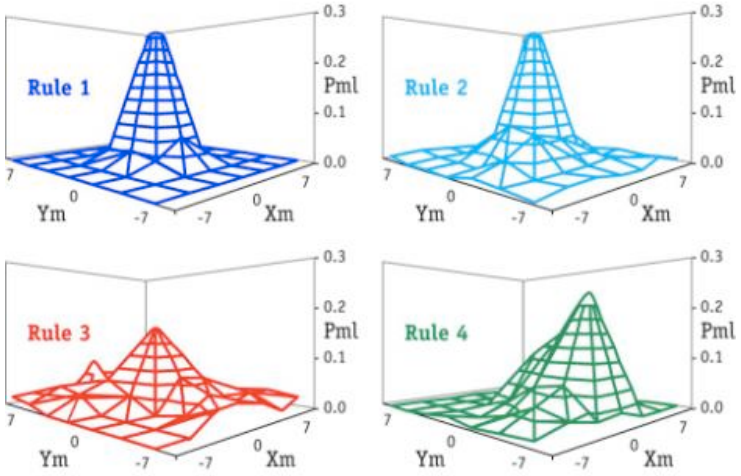

The three-dimensional surface plots of the marble location probability (Pml) for Rules 3 and 4 (lower panel, Fig. 11) confirm the possibility of outlying observations, heterogeneity and non-normality that the Q-Q plots for Rules 3 and 4 show (lower panel, Fig. 10). Again, the distribution one must talk of is the bivariate normal because Xm and Ym are two different vari-

ables. But the results Rules 3 and 4 produce do not look like anything close to a bivariate normal distribution (lower panel, Fig. 11).

As Rule 3 makes the marble rest points move away farther and farther in opposite direction from the (0, 0) target, Pml gets low near the target and fat at the tails of its would-have-been bivariate normal distribution. Indeed, the Rule 3 Pml shows much more dispersion than one would expect to see in a bivariate normal distribution (lower left, Fig. 11). This reconfirms the variance heterogeneity that the parallel boxplot on the lower left of Fig. 9 shows.

Similarly, Rule 4 moves the marble rest points farther and farther from the target as if executing a random walk. Consequently, Pml shifts toward a right skew, showing a long, big, fat tail to the right (lower right, Fig. 9). This corroborates Sparks & Field's (2000, p. 293) prediction that Pml will rise proportionally with each marble drop as the aim for each drop depends on where the marble came to a rest at the previous drop.

Theil's inequality statistics (TIS)

Sparks & Field's (2000, p. 298) recommendation to use residual (error) plots to detect processes that wander prompts Theil's (1966) inequality statistics (TIS). TIS use the *mean square error* (MSE), which measures the average error between competing data series in the same units as the variable itself and weights large errors much more heavily than small ones. TIS provide an elegant decomposition of the MSE into three components: bias (U^M), unequal variation (U^S) and unequal co-variation (U^C), so that $U^M + U^S + U^C = 1$.

Bias arises when competing data have different means. Unequal variation implies that the variances of two time series differ. Unequal covariation means imperfectly correlated data that differ point by point. Dividing each component by the MSE gives the MSE fraction due to bias (U^M), due to unequal variation (U^S) and due to unequal covariation (U^C).

A large U^M reveals a potentially serious systematic error. U^S errors can be systematic too. When unequal variation dominates the MSE, the data match on average and are highly correlated but the variation in two time series around their common mean differs. One variable is a stretched out version of the other. U^S may be large either because of trend differences, or because the data have the same phasing but different amplitude fluctuations (Sterman 2000, p. 876).

If most of the error is concentrated in unequal covariation, then the data means and trends match but individual data points differ point by point. When U^C is large, then most of the error is unsystematic and, according to Sterman: «a model should not be faulted for failing to match the random component of the data» (2000, p. 877).

Figure 12 shows Theil's inequality statistics for Rules 2 through 4 compared to Rule 1, Rule 1 being a process in control with common-cause or random variation. The Xm time series data used for the three-dimensional TIS column chart of Fig. 12 are the same with those used for the Fig. 4 phase plots and the *R* and $\bar{x}$ charts of Fig. 5 and Fig. 6. Overall, moving from the Rule 2 *vs*. Rule 1 to Rule 3 *vs*. Rule 1 to Rule 4 *vs*. Rule 1 comparisons, TIS discount the randomness in the funnel experiment and ascribe the MSE fraction to increasingly rising systematic error.

Specifically, most of the Rule 2 *vs*. Rule 1 MSE fraction soars above unequal variation U^S, with a still large remaining MSE fraction over unequal covariation U^C. The MSE fraction over U^C shows that the Rule 1 and Rule 2 grand means match, but the individual data points these rules produce differ point by point, showing a possibility of unsystematic, i.e., random, error. But the larger MSE fraction over unequal variation U^S shows systematic error: the Rule 1 and Rule 2 sample means are the same, but much more dispersion characterizes Rule 2 than Rule 1.

Figure 12 TIS for Rules 2 through 4 compared to Rule 1 ($U^M + U^S + U^C = 1$)

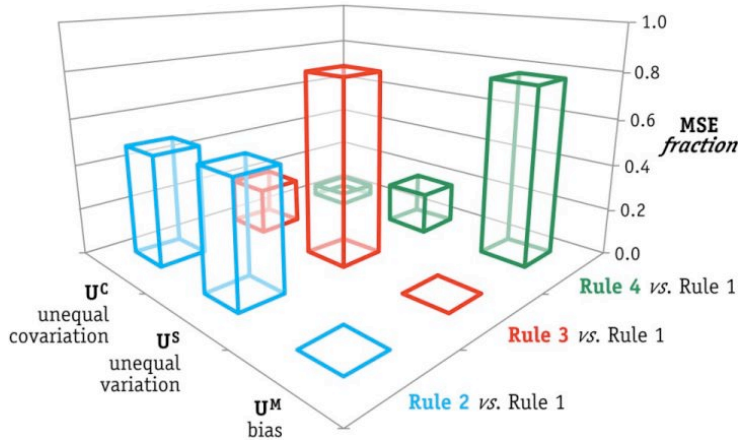

The Rule 2 *vs*. Rule 1 comparison of Fig. 12 supports Sparks & Field's answer to quality practitioner **Question 1** (Table 1b). The SPC charts hug their centerline because tampering Rule 2 causes the large unequal variation U^S that TIS pick up and which translates into the large variance that inflates the *R* and $\bar{x}$ chart control limits (top right, Fig. 5 and Fig. 6). Still, what causes the large variance under tampering Rule 2? How does the structure of relations among variables in the funnel experiment system give rise to its assumption-violating dynamics?

Similar to the Rule 2 *vs*. Rule 1 comparison, most of the Rule 3 *vs*. Rule 1 MSE fraction again ascends above unequal variation U^S, but the remaining MSE fraction over unequal covariation U^C is now smaller than before. The small MSE fraction over unequal covariation U^C shows that the Rule 3 and Rule 1 grand means match, yet the sample means these rules produce differ point by point, again showing possible unsystematic error. The large remaining MSE fraction over unequal variation U^S shows systematic error: the Rule 1 and Rule 3 sample means match, but Rule 3 creates more dispersion than Rule 3 and much, much more than Rule 1.

These results further support Sparks & Field's answer to **Question 2** (Table 1b). The Rule 3 $\bar{x}$ chart hugs the centerline even more because the variance of tampering Rule 3, which inflates the SPC chart control limits, is so large compared to the stable Rule 1 variance that TIS pick it up as serious systematic error. Yet, how does the large variance under tampering Rule 3 happen? What causes it? How do the relations among the funnel system variables cause behaviors that violate Sparks & Field's normality assumptions?

Moving on to the Rule 4 *vs*. Rule 1 comparison of Fig. 12, the 3D TIS column chart tells an entirely different, serious systematic error story. The high U^M MSE fraction shows that the data Rules 1 and 4 generate differ far beyond unequal variation. The competing Rule 4 *vs*. Rule 1 process data have different means. Once more, TIS corroborate Sparks & Field's answer to **Question 5**: the larger the number of marble drops under Rule 4, the more the $\bar{x}$ chart centerline or process mean will differ from the Rule 1 zero target. But what is it that causes such a large variance under Rule 4 that the process mean shifts?

An entropy-based view of tampering

In response to Sparks & Field's (2000, p. 298) concern about the increasing $\bar{x}$ value uncertainty as marble drops increase, the model computes marble location uncertainty (Uml) after each drop dynamically, using Shannon's entropy (uncertainty) formula (Eq. 1). Typically, as marble drops increase, average Uml increases until it saturates at its maximum value of one. The more times

the marble drops through the funnel, the more its final rest points disperse throughout the 7□7 tilling grid, the higher average Uml grows (Fig. 13).

Initially, average Uml is zero and it starts rising as the marble drops increase, coming to a rest randomly around the (0, 0) target. It takes a few marble drops until the tampering Rules 2 through 4 take their toll. Until then, as if uncoupled from Deming's tampering rules, the average Uml behavior is identical for all four rules. After the first few drops, however, tampering begins to show. Uncertainty about the marble's location increases rapidly, its final landing points now guided by Deming's tampering rules. Average Uml continues to rise, but does so at a lower rate for Rule 1 than for Rules 2 through 4 (Fig. 13).

Figure 13 Average marble location uncertainty (Uml) for Rules 1 through 4 (500 drops per rule)

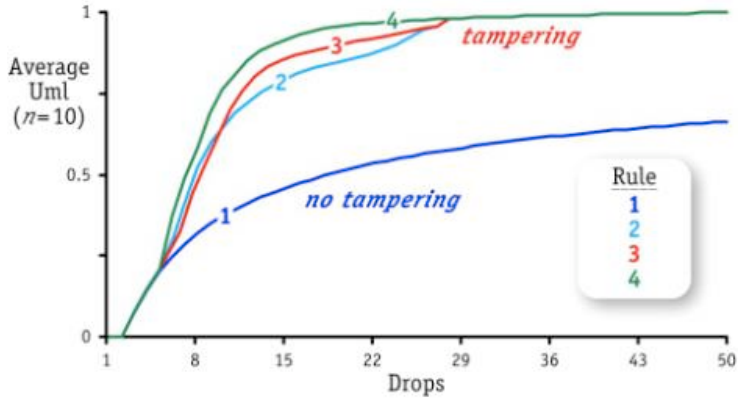

Even if sequestered, there is some uncertainty about the marble's location when Rule 1 plays. When Rules 2 through 4 play, however, average Uml rises rapidly and concomitantly, quickly reaching for its maximum value of one. Under Rules 2 through 4, average Uml is already very close to its saturation point before marble drop 30. But, without tampering, despite its randomness, process Rule 1 continues to sequester the entropy/uncertainty about the marble's whereabouts long past marble drop 30 (Fig. 13).

Feedback loop structure

How structure causes behavior

Figures 14 though 17 revisit the model's funnel (Xf, Yf) and marble (Xm, Ym) location sector (Fig. 2) to show how the feedback-loop structure of relations among variables in the funnel experiment system causes its dynamics. Phase plots highlight the causal relations among the specific variables embedded in feedback loops and confirm loop polarity. Both the funnel and the marble X and Y location dimensions are in perfectly symmetrical feedback loops, so Fig. 14 through 17 show relations (arrow links) that involve the Xf (funnel X coordinate) and Xm (marble X coordinate) dimensions only.

Rule 1 (no tampering) entails one single feedback loop (Fig. 14). Its structure depicts the process of first marking the Xm coordinate where the marble comes to a rest and then purging its value since consecutive marble drops are independent. The Xm stock and the pulse Xm outflow are the two variables embedded in this compensating (negative) feedback loop, its negative pulse Xm-Xm arrow link so marked on Fig. 14 because the link emanates from an outflow. System dynamics accepts this *causal loop* or *influence diagramming* (ID) convention because link polarities depict system ***structure***, not behavior (Richardson 1995; Sterman 2000, p. 139).

Parenthetically, positive (+) links left unmarked is another ID convention. But the loop's behavior depends on conditions set outside the Xm-pulse Xm loop. Namely on change Xm, an inflow that in turn depends on the product of random angle by random distance. Their product adds bipolar (+/–) random input to the change Xm inflow, which in turn feeds the Xm stock. The three phase plots on the top right of Fig. 14 confirm the bipolar random behavior of the three positive causal links outside the Xm-pulse Xm loop. They turn the negative Rule 1 loop positive as the two phase plots on the lower right of Fig. 14 show.

Figure 14 The marble X coordinate (Xm) feedback loop with phase plots for Rule 1 (200 drops)

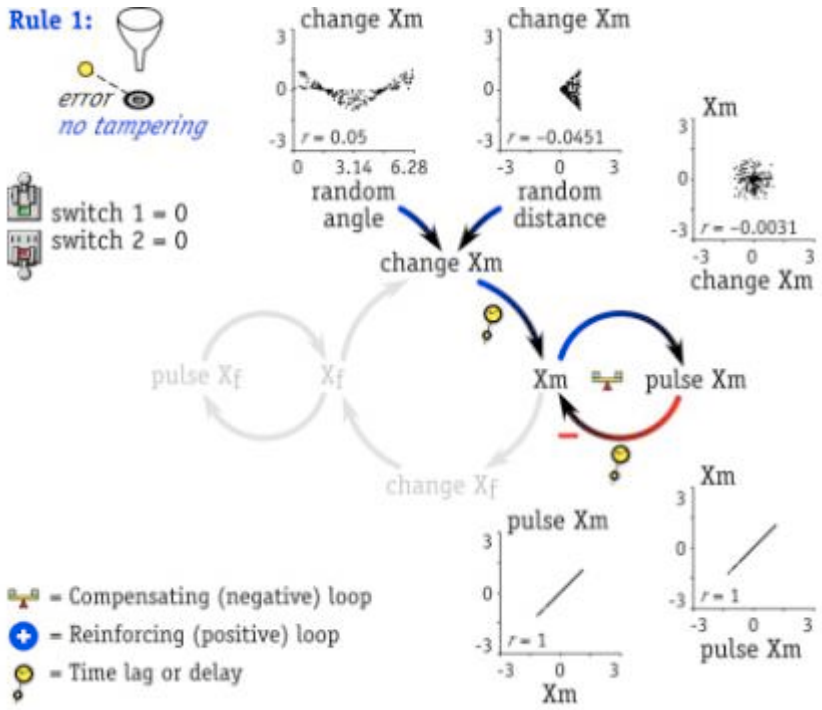

The Xm-pulse Xm feedback loop is negative because it compensates for the random input it receives. And does so both consistently and successfully, not only for Rule 1, but also for Rules 2 through 4. As the marble drops increase, however, its random input turns the negative Xm-pulse Xm loop positive: the more the loop compensates for the bipolar random input it receives, the more it ends up reinforcing its component variables, Xm and pulse Xm, to move in the same direction.

This is an interesting first-order feedback loop that the no tampering Rule 1 of the Deming-Nelson funnel experiment harbors. It makes neither the formal nor the intuitive definitions of loop polarity break off but, rather, an exciting case of shifting loop polarity (Richardson 1995). The phase plots on the lower right of Fig. 14 confirm the ***behavior*** of the Xm-pulse Xm loop as the sign of its stock-*versus*-flow slope, and *vice versa*.

Rule 2 adds a second feedback loop to the structure of relations among variables in the funnel experiment system. The funnel can now move from its last position to compensate for the last error. The change Xf inflow and Xf stock are the new variables embedded in this second compensating (negative) feedback loop. Its Xm-change Xf negative link is so marked on Fig 15 because of the switch 1 = –1 auxiliary converter, which activates the new loop. Switch 2 still equals zero to let the funnel Xf coordinate stock accumulate (Deming's "Memory 1", 2000, p. 328). Formal and intuitive loop polarity definitions notwithstanding, the very purpose of this new

loop, i.e., *to compensate*, gives away its intended dominant polarity, which the phase plots surrounding the influence diagram (ID) of Fig. 15 confirm.

The phase plot on the top left of Fig. 15 shows that the Xf-change Xm link is positive, according to the stock-*versus*-flow slope definition of link polarity. The higher the funnel Xf coordinate stock is, the more its accumulation amplifies the effect of the random angle and random distance product on the change Xm inflow to Xm. The corresponding phase plots on the top middle of Fig. 15 look very different from those on the top middle of Fig. 14. Although still bipolar, neither the *cosine* pattern of random angle nor the *triangular* pattern of random distance effects on change Xm of Fig. 14 are visible on Fig. 15. This is how destructive the tampering of Rule 2 is on the common-cause variation of the funnel experiment.

Figure 15 Funnel X_f and marble Xm feedback loops with phase plots for Rule 2 (200 drops)

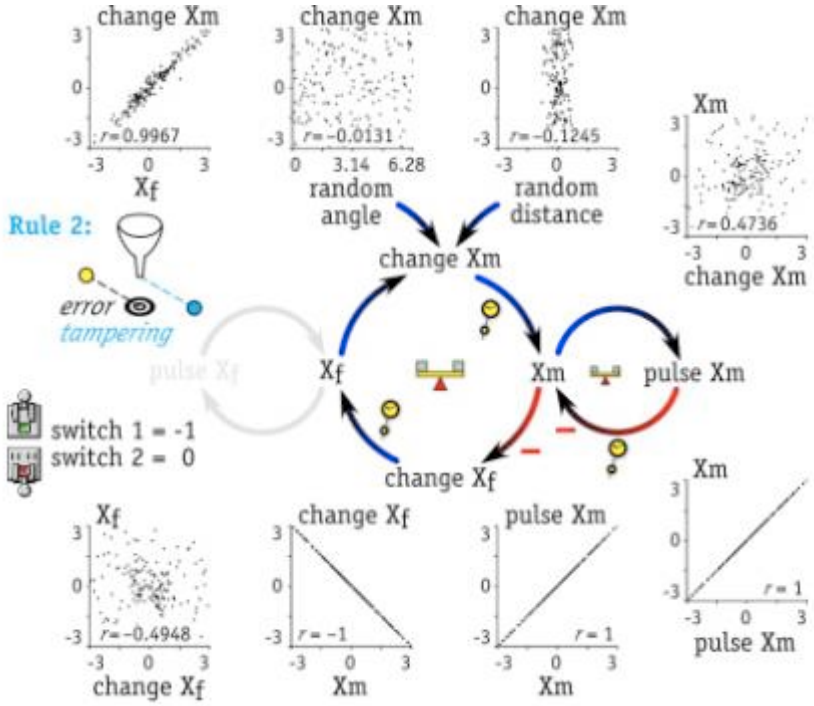

Worth noting on Fig. 15 is how the flow-*versus*-stock phase plots of the change Xm-Xm and change Xf-Xf links are almost symmetrical. Their respective flow-*versus*-stock *correlation coefficient* (*r*) values confirm this almost perfect syzygy (top right and lower left, Fig. 15). But the negative Xm-pulse Xm feedback loop continues to compensate for the amplified bipolar random input it receives as consecutive marble drops stay close to their zero mean. Again, as the marble drops increase, the amplified randomness outside the negative Xm-pulse Xm loop turns it positive (lower right, Fig. 16). The more the Xm-pulse Xm loop compensates for the now tampered with bipolar random input it receives, the more its component variables Xm and pulse Xm move in the same direction, causing the loop's polarity to shift from negative to positive, with a much wider dispersion than Rule 1 did (Fig. 14).

Rule 3 adds a third compensating feedback loop to the structure of relations among the variables in the funnel experiment system (Fig. 16). The purpose of this new negative feedback loop is to bring the funnel back to the (0, 0) target before compensating for the last error (Latzko & Saunders 1995, p. 153). It sounds like zero-based budgeting; does it not? While switch 1 still

equals –1, it is switch 2 = 1 that activates this third feedback loop and prevents the Xf stock from accumulating (Deming's "No memory", 2000, p. 328).

The Xf stock and the pulse Xf outflow are the variables embedded in this compensating (negative) feedback loop, its negative pulse Xf-Xf causal link so marked on Fig. 16 because it emanates from the pulse Xf outflow. The loop's behavior again depends on conditions set outside. Namely on the change Xf inflow that depends on the marble Xm coordinate stock, which in turn depends not only on its pulse Xm outflow, but also on its change Xm inflow (Eq. 2.3, Table 2). Change Xm is itself the sum of the funnel Xf coordinate stock plus the product of random angle by random distance, which adds bipolar (+/–) random input to change Xm. The three phase plots on the top right of Fig. 16 confirm the bipolar random input generated outside the three negative feedback loops of Rule 3. Propagated through the network of positive and negative links of Fig. 16, this bipolar random input turns the negative Rule 3 loop positive as the two phase plots on the left middle show. The *dynamic complexity* that the feedback-loop structure and behavior of the funnel experiment blend can account for the intricate phase plots of the change Xm-Xm and change Xf-Xf causal links (top right and lower left, Fig. 16).

Figure 16 Funnel X_f and marble Xm feedback loops with phase plots for Rule 3 (200 drops)

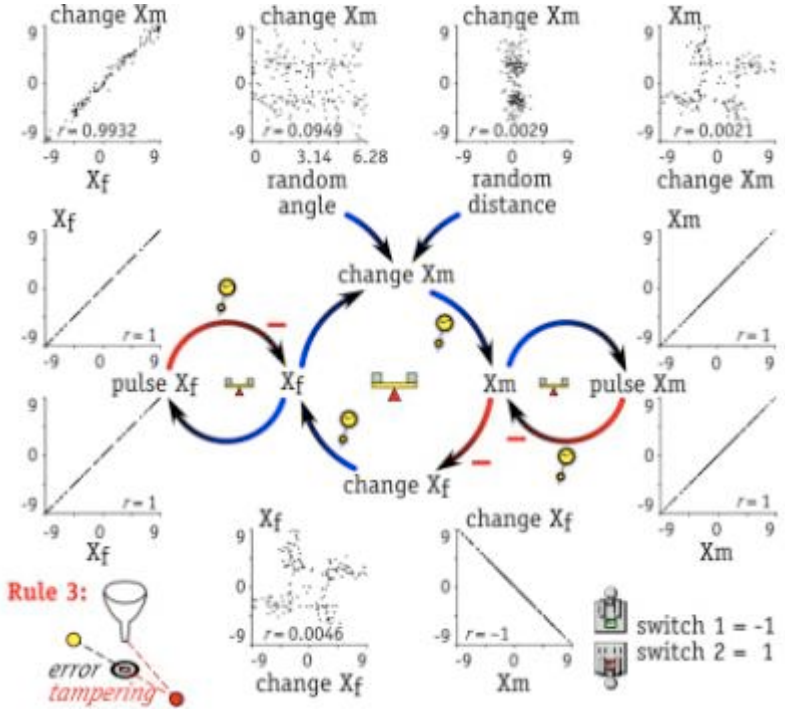

The Xf-pulse Xf feedback loop is negative nonetheless. It compensates for the random input it receives, causing consecutive funnel moves to spread around the (0, 0) target. And does so successfully for Rule 3, but not for Rule 4 (Fig. 17). As the marble drops increase, however, the bipolar random input under Rule 3 turns the negative Xf-pulse Xf loop positive: the more the loop compensates for the bipolar random input it receives, the more it ends up reinforcing Xf and pulse Xf to move in the same direction. This is another interesting first-order feedback loop that Rule 3 of the funnel experiment hides, one more exciting case of shifting loop polarity (Richardson 1995). The phase plots on the left middle of Fig. 16 confirm the behavior of the Xf-pulse Xf loop as the sign of its stock-*versus*-flow slope, and *vice versa*.

Rule 4 does not add a new loop to the structure of relations among variables in the funnel experiment system but turns the compensating feedback loop that Rule 2 added into a reinforcing one (Fig. 17). The purpose? Trying perhaps to cluster marble drops as close as possible, even if away from the (0, 0) target or, as Deming says: "off to the Milky Way" (*cf*. Latzko & Saunders 1995, p. 154). While switch 2 = 1 still prevents the Xf stock from accumulating (no memory), setting switch 1 = 1 changes the polarity of the middle loop from negative (Fig. 16) to positive (Fig. 17). The phase plot on the lower right of Fig. 17 confirms that the Xm-change Xf link turns positive because switch 1 = 1.

Figure 17 Funnel X_f and marble Xm feedback loops with phase plots for Rule 4 (200 drops)

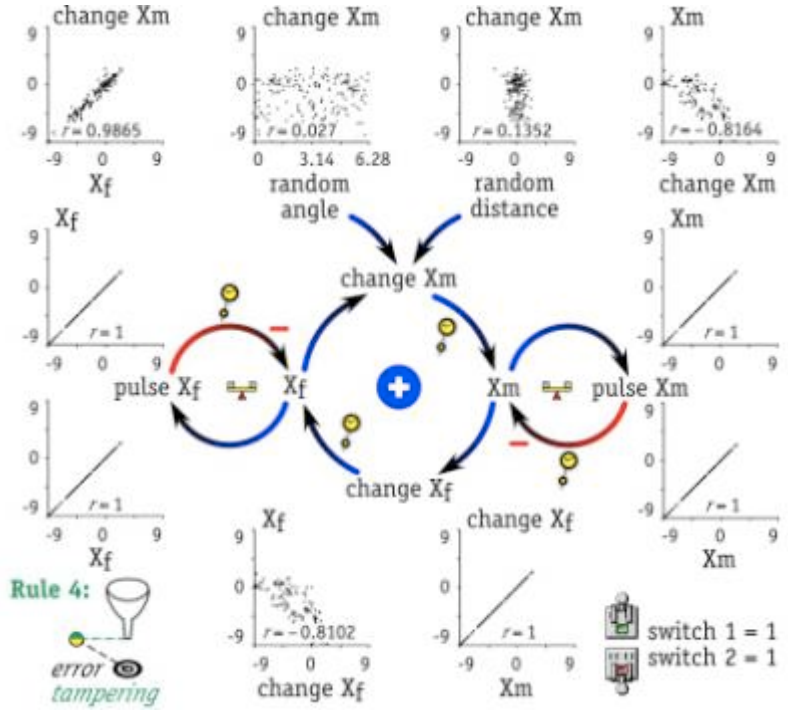

The Xf-change Xm link is again positive under Rule 4 as the phase plot on the top left of Fig. 17 shows. The higher the Xf bias from a previous marble drop, the more it amplifies randomness on the next marble drop. The phase plots on the top middle of Fig. 17 show this off-to-the-Milky-Way bias of Rule 4, which is negative in this instance of the funnel experiment and consistent with the marble location (Xm, Ym) phase plot for Rule 4 (lower right, Fig. 4).

The destructive bias of Rule 4 also shows on the flow-*versus*-stock, symmetrical phase plots of the change Xm-Xm and change Xf-Xf links. Almost in perfect syzygy, their respective negative *r* values confirm the negative, in this instance, bias (top right and lower left, Fig. 17). The negative Xm-pulse Xm loop continues to compensate for the amplified bipolar random input it receives, even though consecutive marble drops no longer stay close to the (0, 0) target. Neither can the compensating Xf-pulse Xf loop cause consecutive funnel moves to stay around the target. As marble drops increase, the now reinforcing middle loop (Fig. 17) amplifies the bipolar random input it receives, making consecutive marble drops and funnel moves behave as if executing a random walk under Brownian motion. The amplification biases the negative Xm-pulse Xm and Xf-pulse Xf loops to compensate away from instead of toward the (0, 0) target.

Answers to quality practitioner questions with system dynamics

The preceding section shows how the structure of relations among variables in the Deming-Nelson funnel experiment system gives rise to its statistical-assumption violating dynamics. It is now possible to add system dynamics insight to answering Questions 1, 2 and 5, marked with the filled diamond symbol ' ' on Table 1b.

Answer to **Question 1**: Rule 2 adds a second feedback loop to the structure of relations among variables in the funnel experiment system. In hopes of hitting the target more, the purpose of this negative feedback loop is to compensate for the last error by letting the funnel move from its last position. The addition of the new negative feedback loop causes common-cause variance amplification. The more the funnel moves from its last position, the more its Xf stock accumulates, the more its accumulation causes dependence among consecutive marble drops and thereby amplifies the randomness associated with each marble drop. The amplified randomness in turn causes the large dispersion that inflates the $\bar{x}$ chart control limits, making it hug the centerline (top right, Fig. 6).

Answer to **Question 2**: Rule 3 adds yet another feedback loop to the structure of relations among variables in the funnel experiment system. Again hoping to hit the target more, this third negative feedback loop brings the funnel back to the (0, 0) target before compensating for the last error. So, it prevents Xf from accumulating. Discarding the funnel's last position before compensating for the last error should take care of the dependence among consecutive marble drops owed to Xf accumulation. Right?

Wrong. The stock and flow structure of the funnel experiment system says otherwise. In trying to decouple dependence due to stock accumulation, the structure of relations among variables under Rule 3 makes consecutive marble drops even more dependent on each other, thereby causing not only a larger dispersion than that of Rule 1 but also variance heterogeneity. The more tightly coupled consecutive marble drops become, the more their dependence amplifies the common-cause variance associated with each marble drop, causing again large and now heterogeneous dispersion that inflates the $\bar{x}$ chart control limits even more than under Rule 2. So it hugs the centerline even more (lower left, Fig. 6).

Answer to **Question 5**: Rule 4 does not add any new loops to the structure of relations among variables in the funnel experiment system but turns the compensating feedback loop that Rule 2 added (Fig. 15) into a reinforcing one (Fig. 17). Hoping not to hit the target more, but perhaps to cluster marble drops close together, the Rule 4 structure makes the funnel aim at the previous marble rest point, while still preventing the funnel Xf stock from accumulating. Again, having discarded the dependence of consecutive funnel moves owed to Xf accumulation, Rule 4 makes consecutive marble drops even more dependent on one another, thereby causing both a larger dispersion than that of Rule 1 and variance heterogeneity.

Worse yet, purposefully reinforcing the randomness associated with each marble drop causes the marble rest points to gradually build a bias, moving in a single direction away from the target as if under Brownian motion. The random component of the funnel experiment stays consistently exogenous to its deterministic causal loop structure but, apparently, the resolute shift in loop polarity now changes the funnel experiment system goal (Richardson 1995).

Conclusion

Enhancing SPC with system dynamics? Clearly, combining these two fields of scientific inquiry can help detect, explain and prevent tampering with the processes managers must manage. When

managers react to variation due to common causes as if it were due to a special cause, two very regrettable outcomes become certain. *First*, their tampering degrades the process and the results are more variable than if the process had been left alone. *Second*, tampering makes it impossible to identify the common causes of variation, leaving no information about how the process can improve. Sometimes variation can be reduced, by understanding what is causing it in a particular situation. Vibration can be damped or prevented, for example, tools can be sharpened more often, worn parts can be adjusted or replaced, and so on. In other cases, however, such as in customer requirements or student interests, variation can be accommodated because is welcome. But to deal appropriately with variation, one must first understand it.

Most managers use, for example, the words 'accurate' and 'precise' as if they were the same. But quality practitioners distinguish between these two very different quality aspects. Imagine an archery student and a target set up at a distance with a clearly marked aim point. Once released, an arrow flies to strike the target. One can measure the distance from the arrow to the aim point to estimate the shot's quality, or the skill of the archer (or the archer's teacher). With only one shot, there is no basis for distinguishing between *precision* and *accuracy*. After several shots, however, say 10, the target's cover has a cluster of 10 holes. Precision measures the dispersion of the results (arrow holes). Low variability equals high precision. Accuracy is the deviation of the center of the group (sample) of holes from the point of aim.

Marks-person trainers also distinguish between these two quality aspects. First, they aim a rifle at a target and clamp it in position. Then, by firing several times, they can measure the average deviation of the rounds from the target and adjust the sights so that the next rounds cluster centers on the target. This is called 'sighting in' a rifle. Marks-persons use the sights consistently to produce as small a cluster as possible. Once they see how rounds clusters deviate on average from the target, they adjust the aim to bring the center of the rounds pattern in line with the target. To improve accuracy, one must not tamper. Improving accuracy is only possible by holding the same aim for a group of rounds and, using the center of their resulting cluster, to estimate the deviation of the entire process of aiming, firing and the rifle and round functioning with the target. Adjusting the aim after each round makes things worse because of the variation endemic to the process.

Back to the funnel experiment. Compared to Rule 1 (no tampering, Fig. 14), the feedback loop structure of tampering Rule 2 (Fig. 15) degrades the precision of the funnel experiment results. The deterministic feedback loop that Rule 2 adds to compensate for the last error from the (0, 0) target amplifies the randomness this negative feedback loop receives exogenously. The more the funnel moves from its last position, the more its Xf and Yf stocks accumulate, the more their accumulation causes dependence among consecutive marble drops (top right, Fig. 8) and thereby amplifies the common-cause variance associated with each marble drop. Accuracy is still high under tampering Rule 2 because the marble rest points' center does not deviate from the point of aim (top right, Fig. 4, 6, 9, 10, and 11).

Compared to Rule 2 (Fig. 15), the feedback loop structure of tampering Rule 3 (Fig. 16) degrades precision even more than Rule 2 does. Hoping to hit the target more, Rule 3 adds a third deterministic feedback loop to the structure of the experiment to bring the funnel back to the target before compensating for the last error and thereby to prevent the funnel Xf and Yf stocks from accumulating. The rationale being that discarding the funnel's last position before compensating for the last error should eliminate dependence among consecutive marble drops owed to Xf and Yf accumulation. Erroneously, however, trying to reduce dependence due to funnel stock accumulation, the structure of tampering Rule 3 makes consecutive marble drops

depend on each other even more than before (lower left, Fig. 8) and thereby degrades precision. The degradation is owed not only to a larger dispersion than that of Rule 1 but also to variance heterogeneity (lower left, Fig. 9). Accuracy again is high under Rule 3 because the marble rest points' center does not deviate from the point of aim (lower left, Fig. 4, 6, 9, 10, and 11).

Compared to Rule 3 (Fig. 16), the feedback loop structure of tampering Rule 4 (Fig. 17) degrades not only precision but also accuracy. Hoping not to hit the target, but to cluster marble drops close together, Rule 4 turns the deterministic, negative feedback loop that Rule 2 added (Fig. 15) into a reinforcing one (Fig. 17). With the increased dependence of consecutive funnel moves, owed to preventing Xf and Yf from accumulating, on the one hand, Rule 4 makes consecutive marble drops depend on each other even more than before (lower right, Fig. 8). So, it reduces precision by causing both dispersion larger than that of Rule 1 and variance heterogeneity (lower right, Fig. 9). On the other hand, with the funnel Xf and Yf coordinates memoryless, reinforcing randomness causes the marble rest points' center to build a bias away from the point of aim, implicitly changing the goal state of the funnel experiment system (lower right, Fig. 4, 6, 9, 10 and 11).

The tampering dynamics of Rule 4 resembles the situation that managers face when they muddle through. Led by logical incrementalism theorists, they too believe that strategic changes envisioned in the complexity theory literature are unrealistic. So, they simply sidestep the systemic leverage analysis and synthesis necessary in strategy design. Anchored in system dynamics, however, systemic leverage analysis and synthesis can help managers align multiple, system goal aiming tactics that mix action with communication in corporate-, business- and functional-level strategy (Georgantzas & Ritchie-Dunham 2002).

Complexity theory and the exponential increase in computational power make simulation a critical fifth tool in addition to the four tools used in science: observation, logical/mathematical analysis, hypothesis testing and experiment (Turner 1997). Simulation modeling with system dynamics permits organization researchers and practitioners to examine the aggregate, dynamic and emergent implications of the multiple, nonlinear, generative mechanisms embedded in the processes capabilities and resources of every modern organization (e.g., Oliva & Sterman 2001 and Repenning & Sterman 2002). Together, SPC and system dynamics can help detect, explain and prevent tampering and its negative effects, which include precision and accuracy degradation in organizational processes. Complementing statistics with system dynamics can help managers sequester the entropy (uncertainty) of the processes they must manage.

Acknowledgement: We are grateful to Dr. Gipsie B. Ranney for her invaluable suggestions that have helped improve this paper immensely.

References

August M, Barovick H, Bland EL, Buia C et al. 2002. Gene tampering. *Time* **160**(16, New York, NY, USA, Oct. 14): 27.

Beck M, Hagar M, LaBreque R, Monroe S & Prout L. 1982. The Tylenol Scare. *Newsweek* (Oct. 11).

Deming WE. 2000a. *Out of the Crisis* (3e). MIT Press: Cambridge, MA. Originally published in 1982 by MIT's Center for Advanced Engineering Study (CAES): Cambridge, MA (Monte Carlo experiments with the funnel, pp. 327-332).

Deming, WE. 2000b. *The New Economics for Industry, Government, Education* (2e). MIT Press: Cambridge, MA. Originally published in 1993 by MIT's Center for Advanced Engineering Study (CAES): Cambridge, MA (Ch. 9: The Funnel).

Dobbs L. 2002. Toothless tigers. *Money* **31**(9, Sep.): 63-64.

Field JBF & Sparks RS. 1995. Why do my control charts look funny? Answer: Check the assumptions. *The Quality Magazine* **4**: 81-84.

Forrester JW. 1958. Industrial dynamics: A major breakthrough for decision makers. *Harvard Business Review* **36**(4): 37-66.

Forrester JW. 1961. *Industrial Dynamics*. MIT Press: Cambridge, MA (currently available from Pegasus Communications: Waltham, MA).

Georgantzas NC. 2002. Play with the ants to understand CASOS. In *Proceedings of the* 20*th International System Dynamics Society Conference*, July 28 - August 1, Villa Igiea, Palermo, Italy.

Georgantzas NC & Acar W. 1995. *Scenario-driven planning: Learning to manage strategic uncertainty*. Greenwood/ Quorum: Westport, CT.

Georgantzas NC & Ritchie-Dunham JL. 2002. Designing high-leverage strategies and tactics. *Human Systems Management* **21**(4): 217-227.

Grubbs, FS. 1983. An optimum procedure for setting machines. *Journal of Quality Technology* **15**(4): 155-208.

Gunter B. 1993. Through a funnel slowly with ball bearing and insight to teach experimental design. *The American Statistician* **47**: 265-269.

Latzko WJ & Saunders DM. 1995. *Four Days with Dr. Deming: A Strategy for Modern Methods of Management*. Addison-Wesley: Reading, MA (Ch. 9: The Funnel, pp. 147-155).

MacGregor, JF. 1990. A different view of the funnel experiment. *Journal of Quality Technology* **24**: 255-259.

Merriam-Webster's Collegiate Dictionary (10e). 2001. Merriam-Webster, Inc.: Springfield, MA.

Mintzberg H. 1994. *The Rise and Fall of Strategic Planning*. Free Press: New York, NY.

Mitroff II & Kilmann RH. 1984. *Corporate Tragedies: Product Tampering, Sabotage and Other Catastrophes*. Praeger Publishers: New York, NY.

O'Connor CM. 2002. Class-action lawsuits target IPO laddering. 2002. *Investor Relations Business* (Jul. 1): 1.

Oliva R & Sterman JD. 2001. Cutting corners and working overtime: Quality erosion in the service industry. *Management Science* **47**(7): 894-914.

Quinn JB. 1980. *Strategies for Change: Logical Incrementalism*. Irwin: Homewood, IL.

Repenning NP & Sterman JD. 2002. Capability traps and self-confirming attribution errors in the dynamics of process improvement. *Administrative Science Quarterly* **47**: 265-295.

Richardson GP. 1995. Loop polarity, loop dominance and the concept of dominant polarity. *System Dynamics Review* **11**(1): 67-88.

Richmond B et al. 2001. *iThink Analyst* 7: *The power to understand!* High Performance Systems, Inc.: Hanover, NH.

Richmond B. 1980. A new look at an old friend. *Plexus*. Hanover, NH: Dartmouth College.

Schultz LE. 1994. *Profiles in Quality: Learning from the Masters*. Quality Resources (A Division of The Kraus Organization Ltd.): White Plains, NY.

Shannon CE & Weaver W. 1949 *The Mathematical Theory of Communication*. University of Illinois: Urbana, IL.

Shewhart WA. 1980. *Economic Control of Quality of Manufactured Product* (50th Anniversary Commemorative Issue/No H 0509). ASQ: Milwaukee, WI. Originally published in 1931 by Van Nostrand: New York, NY.

Sparks RS & Field JBF. 2000. Using Deming's funnel experiment to demonstrate effects of violating assumptions underlying Shewhart's control charts. *The American Statistician* **54**(4): 291-302.

Sterman JD. 2000. *Business Dynamics: Systems Thinking and Modeling for a Complex World*. Irwin McGraw-Hill: Boston, MA.

Sterman JD. 2001. System Dynamics Modeling: Tools for learning in a complex world. *California Management Review* **43**(4, Summer): 8-25.

Theil H. 1966. *Applied Economic Forecasting*. Elsevier Science (N. Holland): New York, NY.

Turner F. 1997. Foreword: Chaos and social science. In RA Eve, S Horsfall & ME Lee (Eds). *Chaos, Complexity and Sociology*. Sage: Thousand Oaks, CA (pp. xi-xxvii).

Wheeler DJ. 2000. *Normality and the Process Behavior Chart*. SPC Press: Knoxville, TN.

Wilk MB & Gnanadesikan R. 1968. Probability plotting methods for the analysis of data. *Biometrika* **55**: 1-17.

Back to the Top